

# Characterization of Ce<sup>3+</sup> doped ZnO nano-powders co-doped with Eu<sup>3+</sup> in PVC polymer films

MA Malimabe<sup>1</sup>, LF Koao<sup>1</sup>, HC Swart<sup>2</sup>, K Von Eschwege<sup>2</sup> and JS Sefadi<sup>3</sup>

<sup>1</sup>Department of Physics, University of the Free State (Qwa Qwa Campus), Private Bag X13, Phuthaditjhaba, 9866, South Africa

<sup>2</sup>Department of Physics /Chemistry, University of the Free State, P.O. Box 339, Bloemfontein, 9300, South Africa.

<sup>3</sup>Department of Chemistry, Sol Plaatje University, Private Bag X1001, South Africa

E-mail: mokoename@ufs.ac.za

**Abstract.** Nanoparticles of ZnO and Ce<sup>3+</sup> doped ZnO co-doped with Eu<sup>3+</sup> were synthesized by the chemical bath deposition method (CBD) and spread through poly (vinyl chloride) (PVC) polymer matrix via the solution casting method. The optical properties of these polymer based Ce<sup>3+</sup> doped ZnO also co-doped with Eu<sup>3+</sup> nanomaterials were studied. The X-ray diffraction (XRD) pattern for the ZnO flower-like nanostructures showed crystalline peaks corresponding to a hexagonal wurtzite ZnO structures. The diffraction peaks shift towards lower angles with the presence of dopant(s) indicating that dopant ions are well incorporated into the lattice sites of Zn<sup>2+</sup>. Scanning electron microscope (SEM) showed that ZnO nanoparticles were found to spread more homogeneously in the PVC matrix. Parameters such as transmittance and reflectance were determined with a UV-vis spectroscope. UV-Vis spectra of the polymer films showed a slight red-shift when the ZnO was singly doped with Eu<sup>3+</sup> and Ce<sup>3+</sup>, respectively. However, there was a blue shift for the co-doped nanocomposite. The photoluminescence results showed that the polymer films exhibited a luminescence band around 444 nm. Eu<sup>3+</sup> in the co-doped nano-powders brought about an increase in the luminescence intensity. A maximum intensity was found when 1 mol % of Eu<sup>3+</sup> was incorporated in the PVC.

## 1. Introduction

Luminescent nanoparticles are used in many fields of applications, such as bio-imaging, nano-sensors as well as in light emitting diodes [1, 2]. Recently, white light emitting diodes (LED's) have been attracting a great deal of attention in solid state lighting due to their favorable characteristics such as long lifetime, lower energy consumption, higher reliability and environment-friendly affiliation. Zinc oxide (ZnO) is a wide band gap n-type semiconductor (3.33 eV) and also have high exciton binding energy at room temperature [1, 3]. Wide band gap materials always present good potential for full color phosphor and ZnO is one of the wide band gap materials with versatile applications. ZnO crystallizes in two main forms, namely; hexagonal wurtzite, which is formed under more general conditions, and cubic zinc blende. ZnO has remarkable performance in electronics, optics and photonics which make it attractive for many applications such as UV lasers, light emitting diodes, solar cells, Nano generators, gas sensors, photodetectors and photo catalysts [2, 3]. Previous attempts at doping ZnO nano-structures frequently yielded inhomogeneous doped materials. The frequent failure of which was attributed to the expulsion of dopant ions to the surface of nanocrystals by the intrinsic process of self-annealing or the ability of the ion to adsorb to the exposed surfaces of the nanocrystals. The attempt to achieve successful doping of nanocrystals can be through involving nanocrystals of the right size and morphology and choosing surfactants that do not bind too strongly to

the dopant ions. Lately, the incorporation of polymer nanofibers in rare earth metal doped nanocrystals has been investigated [4, 5]. Polymers doped with rare earth ( $RE^{3+}$ )  $\beta$ -diketonate complexes have attracted considerable interest because they preserve the luminescence properties of the complexes while they can be processed from solution and are mechanically flexible [4, 5]. Polymers such as PMMA and PET possess many desirable properties, such as high light transmittance, chemical resistance, colourless, resistance to weathering corrosion, good insulating properties, low optical absorption, refractive index tailorability with molecular weight, simple synthesis, and low cost. These characteristics make them suitable as a host material for  $RE^{3+}$  ions and organic dye doping [5, 6]. Strong  $Eu^{3+}$  ion red emission and almost no defect emission from ZnO obtained by uniformly dispersing  $Eu^{3+}$  ion doped ZnO nanocrystals in a polymer hybrid nanofiber [7, 8]. The strong red emission was attributed to the small crystal size, embedded ZnO nanocrystals in Polymer (PVA) and  $-OH$  group bonding [9, 10]. These findings open room for further study in that one can choose different polymers to realize various and specialized functionalities.

The project therefore focuses on possibility of engineering band gap and influencing physical, chemical and optoelectronic properties of ZnO by varying the dimensions of the system and changing the diameters as well as the composition of nanostructures. The ZnO, ZnO doped:  $Ce^{3+}$  and  $Eu^{3+}$ , and ZnO co-doped with  $Ce^{3+}$  and  $Eu^{3+}$  respectively, nanostructures with various sizes, shapes and compositions dispersed in polymer matrix of PVC, PCL (polycaprolactone) and PVC/PCL blend respectively are studied with different techniques, including photoluminescence (PL) spectroscopy. The paper reports on these nanoparticles dispersed in PVC matrix.

## 2. Experimental

*Materials synthesis:* All the chemicals used for the preparation of the powders were of analytical grade. It includes zinc acetate ( $Zn(CH_3COO)_2 \cdot 2H_2O$ ), cerium acetate ( $Ce(CH_3CO_2)_3 \cdot xH_2O$ ), thiourea ( $(NH_2)_2CS$ ) and ammonium oxide ( $(NH_4)_2O$ ). All the precursors were dissolved in deionized water. During the preparation of the powders, ammonia was used as a complexing agent. The amount of each solution was taken in the following order: 60 mL of zinc acetate was first placed in the water bath at 80 °C, followed by addition of 60 mL of thiourea and the ammonium oxide was then added dropwise in the mixture, while continuously stirring for  $\pm 10$  minutes then left overnight at room temperature. The deposit was then vacuum filtered and washed with distilled water and left to dry at ambient temperature. The powders were then annealed in the furnace at 700 °C for 2 hours. 0.5 g Poly (vinyl chloride) and 0.03g powders were dissolved in 10 mL acetophenone. The polymer solution was then casted in an evaporating dish and left to dry. The particle size, morphology and the structural and optical properties of the as-synthesized samples were analysed by means of Scanning electron microscopy (SEM), Elemental energy dispersive analysis (EDS), X-ray diffraction (XRD), UV-vis spectroscopy and photoluminescence (PL).

## 3. Results and Discussion

### 3.1. Structural analysis

*3.1.1. X-ray diffraction analysis:* XRD analysis was carried out in order to study the structural properties of the ZnO powders, undoped and ZnO:  $Eu^{3+}$ , ZnO:  $Ce^{3+}$  and ZnO:  $Ce^{3+}$ :  $Eu^{3+}$  doped. Figure 1 (a) shows the XRD patterns of the ZnO powders synthesized by CBD. All the diffraction peaks located at  $2\theta$  values between 30° to 70° are well consistent with the hexagonal wurtzite crystal structure (JCPDS 75-0576). Figure 1(b) illustrates the XRD patterns of ZnO, ZnO:  $Eu^{3+}$ , ZnO:  $Ce^{3+}$  and ZnO:  $Ce^{3+}$ :  $Eu^{3+}$  powders in the PVC polymer matrix. The XRD patterns of the all the PVC films

show the characteristic peaks of PVC at  $2\theta$  between  $17.5^\circ - 25^\circ$  (JCPDS 15-09999) [11]. The characteristic XRD patterns of the PVC films also shows the presence of the hexagonal wurtzite structure of ZnO powders in Figure 1(b). Figure 2 illustrates the diffraction patterns of peak 101 for (a) all undoped, doped and co-doped ZnO powders and (b) polymer films with the powders distributed within the polymer matrix. The diffraction peaks shift towards lower angles with the presence of dopend(s). This shift is more evident with  $\text{Eu}^{3+}$  ion than  $\text{Ce}^{3+}$  ions in  $\text{ZnO}:\text{Ce}^{3+}$ . The peak intensity decreased for all the singly doped ZnO powder and there is a slight increase in diffraction intensity with  $\text{Eu}^{3+}$  co-doping. The latter observation is the indication that the lattice parameters are slightly larger in  $\text{ZnO}:\text{Ce}^{3+}:\text{Eu}^{3+}$  co-doped than singly doped and those of undoped ZnO [12]. The peak shift is the evidence that  $\text{Eu}^{3+}$  and  $\text{Ce}^{3+}$  have larger radii than  $\text{Zn}^{2+}$  in the range (0.095 nm, 0.1034 nm and 0.074 nm). This is also an indication that  $\text{Eu}^{3+}$  ions are well incorporated into the lattice sites of  $\text{Zn}^{2+}$  which leads to an increase in inter atomic distances. Crystallite size of the nanoparticles were estimated from the full width at half-maximum (FWHM) using the Debye -Scherrer formula [12]. The estimated crystallite sizes are 57, 64, 53 and  $85 \pm 1$  nm respectively for ZnO, ZnO:  $\text{Eu}^{3+}$ , ZnO:  $\text{Ce}^{3+}$  and ZnO:  $\text{Ce}^{3+}:\text{Eu}^{3+}$  powders.

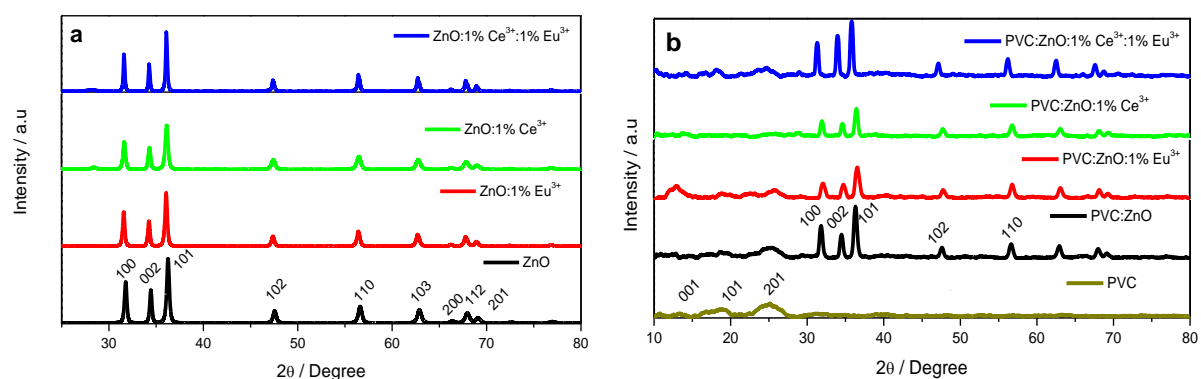


**Figure 1.** XRD patterns of (a) ZnO, ZnO:  $\text{Eu}^{3+}$ , ZnO:  $\text{Ce}^{3+}$  and ZnO:  $\text{Ce}^{3+}:\text{Eu}^{3+}$ , nano-powders (b) ZnO, ZnO:  $\text{Eu}^{3+}$ , ZnO:  $\text{Ce}^{3+}$  and ZnO:  $\text{Ce}^{3+}:\text{Eu}^{3+}$  nano-powders in the PVC polymer matrix.

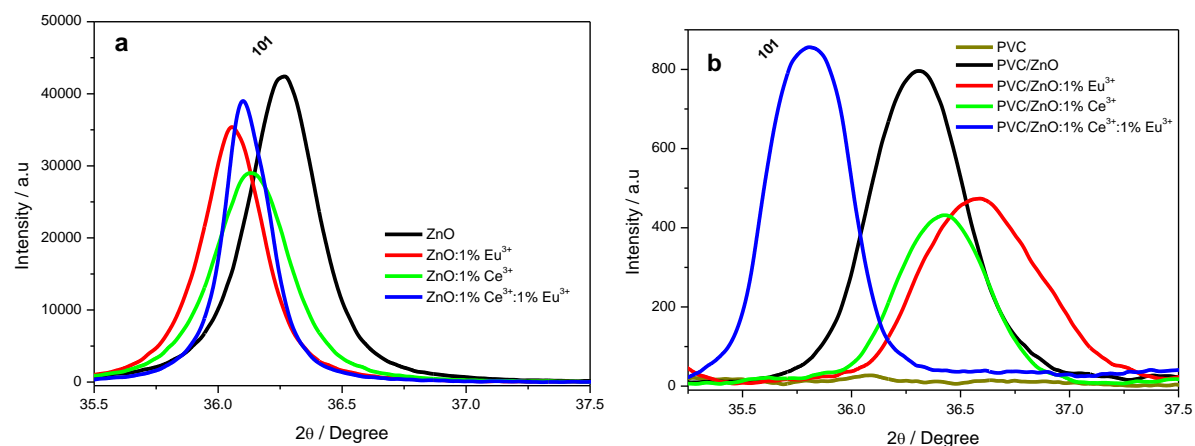


**Figure 2.** (a) Diffraction pattern (101) for (a) ZnO, ZnO:  $\text{Eu}^{3+}$ , ZnO:  $\text{Ce}^{3+}$  and ZnO:  $\text{Ce}^{3+}:\text{Eu}^{3+}$  and (b) PVC films filled with ZnO, ZnO:  $\text{Eu}^{3+}$ , ZnO:  $\text{Ce}^{3+}$  and ZnO:  $\text{Ce}^{3+}:\text{Eu}^{3+}$  nano-powders.

The diffraction patterns of polymer films of ZnO powders undoped, doped and codoped with  $\text{Eu}^{3+}$  and  $\text{Ce}^{3+}$  ions are shown in Figure 2(b). There is a shift towards larger angles for ZnO:  $\text{Eu}^{3+}$  and ZnO:  $\text{Ce}^{3+}$  doped powders in PVC matrix and a decrease in the diffraction peak intensity. A considerable shift towards lower angles for ZnO:  $\text{Eu}^{3+}$ :  $\text{Ce}^{3+}$  co-doped PVC film is observed and an increase in the diffraction peak intensity. This observation is in line with the estimated crystal sizes that are respectively  $40$ ,  $32$ ,  $42$  and  $48 \pm 1$  nm for ZnO, ZnO:  $\text{Eu}^{3+}$ , ZnO:  $\text{Ce}^{3+}$  and ZnO:  $\text{Ce}^{3+}$ :  $\text{Eu}^{3+}$  powders in PVC matrix.

**3.1.2. Surface morphological analysis:** Figure 3(a) show SEM images of the as prepared ZnO nanostructures, respectively doped with 1%  $\text{Eu}^{3+}$ , 1%  $\text{Ce}^{3+}$  and co-doped with 1%  $\text{Eu}^{3+}$  and 1%  $\text{Ce}^{3+}$  and annealed at  $700^\circ\text{C}$  for 2 hours. The SEM images shows that nanoparticles assume the flower-like structures of the undoped ZnO with the co-doped nanoparticles more agglomerated than in the singly doped ZnO. The undoped ZnO flower-like particles are non-agglomerated, which makes it evident that co-doping with  $\text{Eu}^{3+}$  and  $\text{Ce}^{3+}$  (D) brings about agglomeration. This is in agreement with the observation from XRD that there is an increase in the particle size in the doped ZnO powders. In Figure 3(b) the nanoparticles are distributed homogeneously within the PVC polymer matrix with the particles of ZnO:  $\text{Ce}^{3+}$  diminishing.

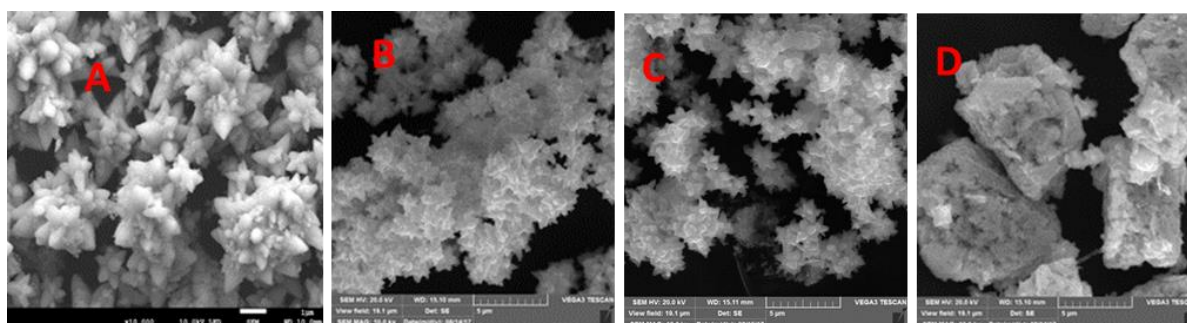


**Figure 3. (a)** SEM images of virgin powders (ZnO, ZnO:  $\text{Eu}^{3+}$ , ZnO:  $\text{Ce}^{3+}$  and ZnO:  $\text{Ce}^{3+}$ :  $\text{Eu}^{3+}$ )

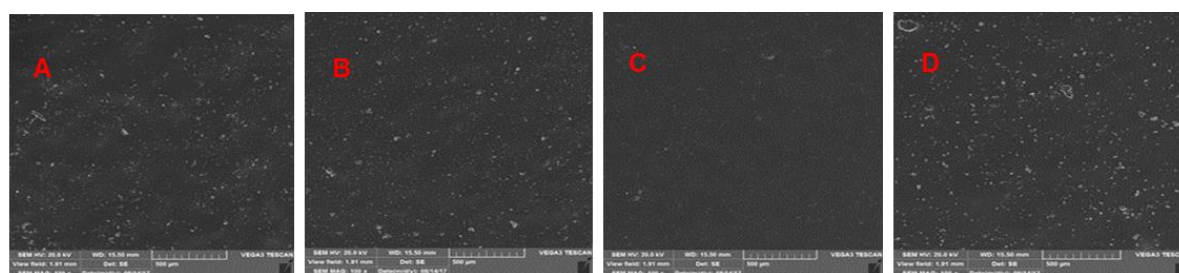


**Figure 3. (b)** SEM images of powders (A) ZnO, (B) ZnO:  $\text{Eu}^{3+}$ , (C) ZnO:  $\text{Ce}^{3+}$  and (D) ZnO:  $\text{Ce}^{3+}$ :  $\text{Eu}^{3+}$  in PVC polymer matrix.

### 3.2. Optical properties

The UV-visible reflectance (dotted) spectra of the ZnO, ZnO:  $\text{Eu}^{3+}$ , ZnO:  $\text{Ce}^{3+}$  and ZnO:  $\text{Ce}^{3+}$ :  $\text{Eu}^{3+}$  nanoparticles and the PVC polymer films of these nanoparticle are illustrated in Figure 4. The measurements were done at room temperature and normal incident as a function of wavelength in the spectral range from  $200$  nm up to  $800$  nm. The estimated absorption edge of the powders is around

389 nm, which is due to the free exciton from the wide band gap of ZnO (3.33 eV) [3]. Doping and co-doping show no significant effect on the reflectance of the ZnO powders. There is a decrease in the transmittance of ZnO nanopowders when distributed in PVC matrix. A slight increase is observed when ZnO: Eu<sup>3+</sup>: Ce<sup>3+</sup> co-doped nanopowders are in PVC film. The absorption edge shifted slightly to lower wavelengths in powders distributed within the PVC polymer matrix. This blue shift excitation is due to the encapsulation of powders by PVC making the codoped powders to reflect UV light at higher frequencies.

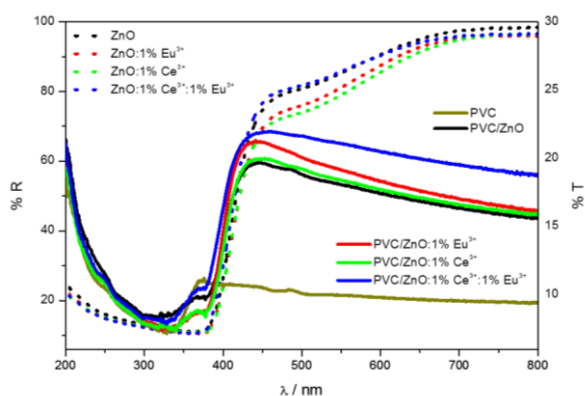


**Figure 4** UV-vis reflectance spectra of (a) ZnO, ZnO: Eu<sup>3+</sup>, ZnO: Ce<sup>3+</sup> and ZnO: Ce<sup>3+</sup>: Eu<sup>3+</sup>, nanopowders as well as the transmittance spectra of ZnO, ZnO: Eu<sup>3+</sup>, ZnO: Ce<sup>3+</sup> and ZnO: Ce<sup>3+</sup>: Eu<sup>3+</sup> nanopowders in PVC polymer matrix

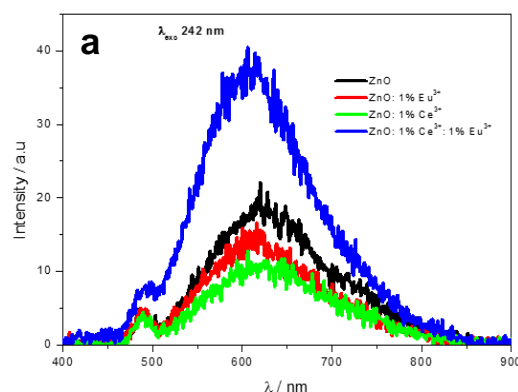


**Figure 5(a)** PL emission spectra of ZnO, ZnO: Eu<sup>3+</sup>, ZnO: Ce<sup>3+</sup> and ZnO: Ce<sup>3+</sup>: Eu<sup>3+</sup> nano-powders

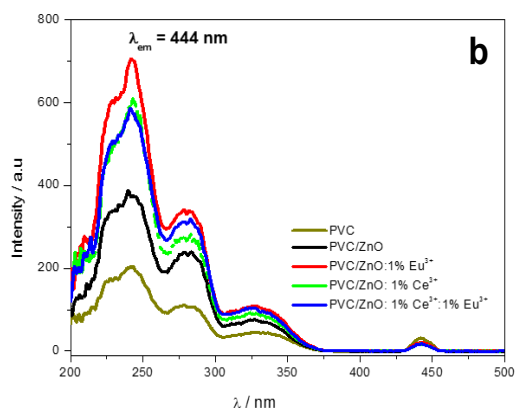
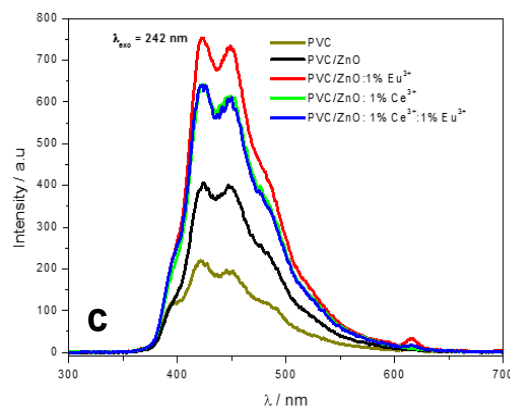


**Figure 5 (b)** PL excitation spectra of (c) PL emission spectra of ZnO, ZnO: Eu<sup>3+</sup>, ZnO: Ce<sup>3+</sup> and ZnO: Ce<sup>3+</sup>: Eu<sup>3+</sup> nano-powders in PVC polymer matrix.



### 3.3. Photoluminescence (PL)

The photoluminescence (PL) measurements was carried out at room temperature using Xenon lamp. The PL excitation and emission spectra of ZnO, ZnO: Eu<sup>3+</sup>, ZnO: Ce<sup>3+</sup> and ZnO: Ce<sup>3+</sup>: Eu<sup>3+</sup> nanopowders and these powders in PVC polymer films are shown in Figure 4(a-c). Figure 4(a) depicts

broad emission spectra for undoped ZnO powders at around 620 nm. There is a decrease in luminescence intensity of singly doped ZnO powders and a significant increase for the co-doped nanoparticles. This increase in intensity may be due to an increase in crystal size, as determined by the XRD results, which enhances luminescence. PL excitation spectra in Figure 5(b) show a broad emission respectively 242 nm, 289 nm, 365 nm and 444 nm due to PVC defect. The photoluminescence results showed that the polymer films exhibited a luminescence band around 444 nm. Eu<sup>3+</sup> ion in the doped nano-powders brought about an increase in the luminescence intensity. This increase is due to the effective interaction between the nanoparticles of Eu<sup>3+</sup> doped ZnO with the PVC matrix. It is evident that ZnO: Ce<sup>3+</sup> powders have the lowest emission intensity when incorporated in PVC film. There is also a shift from the brought peak at 620 nm for powders to much intense peaks of polymer film at 444 nm. The powders emit better when distributed within the polymer matrix than if uncovered. This is an indication that good conductance could be achieved with the use of polymers to distribute doped ZnO powders

#### 4. Conclusion

CBD synthesized nano-powders (undoped and Ce<sup>3+</sup>: Eu<sup>3+</sup> co-doped ZnO) are distributed through the PVC polymer matrix by solution casting. From XRD studies, the hexagonal wurtzite ZnO structure was not altered, however, Ce<sup>3+</sup> ions shifted the peaks to lower 2 $\theta$  (degrees) and quenched the intensity. Results also showed an increase in intensity for the co-doped ZnO incorporated in the PVC polymer matrix. The UV results showed that there was a red shift in the absorption edges with the incorporation of the singly doped powders. An additional red shift was seen in the low mol % Eu<sup>3+</sup> ions of the co-doped nanocomposites. Lastly, this method has the potential for the production of luminescent polymer nanocomposites emitting the basic colors (red, green and blue).

#### Acknowledgement

The author would like to acknowledge the National Research Foundation (UID: 99224) and the University of the Free State for financial support.

#### References:

- [1] Zhang Y, Ram M K, Stefanakoa E K, Goswami Y 2012 *J. Nanomater.* **2012** 1-22
- [2] Sebastian L, Maria J Q, Manuel H G, Alfredo A 2014 *World J. Condens. Matter. Phys.* **4** 227-234
- [3] Molefe F V, Koao L F, Dejene B F, and Swart H C 2015 *Opt. Mater.* **46** 292–298
- [4] Kumar N.B.R, Crasta V, Bhajantri R.F, Praveen B.M 2014 *J. Polym* **2014** 1-8
- [5] Koao L F, Dejene B F, Swart H C, Motloung S V, Motaung T E and Hlangothi S P 2016 *J. Adv. Mater. Lett.* **7** (7) 529-535
- [6] Marimuthu T, Anandhan N, Ravi G and Rajendran S 2014 *J. Nano Sci. and Technol.* **2** 62-65
- [7] Humayun Q, Kashif M and Hashim U 2013 *J. Nanomater* **2013** 1-9
- [8] Mosquera E, del Pozo I, Morel M 2013 *J. Solid State Chem.* **206** 265-271
- [9] Zhang Y, Liu Y, Li X, Wang Q J and Xie E 2011 *Nanotech.* **22** 1-9
- [10] Kamari H M, Al-Hada N M, Saion E, Shaari A H, Talib Z A, Flaifel M H and Ahmed AAA 2017 *Cryst* **7** (2) 1-14
- [11] Da Silva M A, Adeodato Vieira M G, Macumoto A C G and Beppu M M 2011 *Polym. Testing* **30** 478-484
- [12] Koao L F, Dejene B F, Swart H C, Motloung S V, Motaung T E 2016 *Opt. Mater.* **60** 294-304